



# Infrared Vertical Cavity Surface-Emitting Laser barriers to measure movements of freshwater and marine invertebrates

Vittorio Pasquali<sup>1</sup>, Nicola Cosmar<sup>2</sup>, Fabio Leccese<sup>3</sup>

<sup>1</sup> Department of Biology, University of Salento, via Monteroni n.165, 73100 Lecce, Italy

<sup>2</sup> Optek Technology Inc, 2900, E Plano Parkway, Suite 200, Plano, Texas, 75074, United States of America

<sup>3</sup> Science Department, Università degli Studi Roma Tre, via della Vasca Navale n.84, 00146 Rome, Italy

## ABSTRACT

In this article, we present an optical system based on Infrared VCSEL Laser and NPN phototransistor. The output signal of each optoelectronic emitter-receiver couple is managed by a cheap electronic circuit, which ensures high flexibility and the modularity of the various components of the system. At the end of the measurement chain, there is the Raspberry-Pi model 3B+. The aim of the current work was to design a system able to monitor locomotor activity of small marine and freshwater animals: nudibranch *Melibe viridis* and cave decapod *Typhlocaris salentina*. Our results showed that the optical system can detect the movement of small aquatic animals inside medium and big aquaria. From an ethological point of view, these results show that the device can be useful for monitoring the locomotor activity, including long-term monitoring needed to characterize the chronobiological parameters of these animals. In conclusion, we have found the IR-actuated movement detector to be a highly sensitive and reliable device, in spite of its relatively low cost. It is appropriate to a wide range of experiment protocols and data-recording systems.

**Section:** RESEARCH PAPER

**Keywords:** infrared; VCSEL; behaviour; circadian rhythms; locomotor activity journal

**Citation:** V. Pasquali, N. Cosmar, F. Leccese, Infrared Vertical Cavity Surface-Emitting Laser barriers to measure movements of freshwater and marine invertebrates, Acta IMEKO, vol. 14 (2025) no. 4, pp. 1-6. DOI: [10.21014/actaimeko.v14i4.2120](https://doi.org/10.21014/actaimeko.v14i4.2120)

**Section Editor:** Leonardo Iannucci, Politecnico di Torino, Italy

**Received** May 20, 2025; **In final form** August 25, 2025; **Published** December 2025

**Copyright:** This is an open-access article distributed under the terms of the Creative Commons Attribution 3.0 License, which permits unrestricted use, distribution, and reproduction in any medium, provided the original author and source are credited.

**Corresponding author:** F. Leccese, e-mail: [fabio.leccese@uniroma3.it](mailto:fabio.leccese@uniroma3.it)

## 1. INTRODUCTION

The infrared (IR) light has a specific physical property useful when studying animals: it is not seen by those that are not sensitive to these frequencies. Discovered in 1800 by William Herschel, the first IR photoconductor was developed by Theodore Case in 1917, and it was based on the photoconductivity exhibited by a substance composed of thallium and sulphur (Tl<sub>2</sub>S) [1].

Nowadays, behavioural research on the monitoring of locomotor activity is strongly centred around video-analysis systems [2], while infrared (IR) photocells were the core sensors of many commercial and home-made devices from '70 to '90. IR-based methods have several advantages: they are not intrusive, can work with 0 lux, produce output suitable for direct computer analysis, and they adapt to a lot of different conditions.

One of the first applications of IR photocells in behavioural research has been to measure motor activity in rodents, at least since 1970 [3]. This technology has been used in behavioural research to record total distance travelled [4], spatial patterns of

locomotion [5], immobility/freezing [6], hole pokes [7], time spent in specific areas/compartments of the apparatus [8], drinking and eating behaviour [9], non-invasive monitoring of vital parameters [10]–[15], environmental quality [16], [17], as well as food quality [18] and its conservation [19]. Another important application is chronobiological studies, and the IR revealed itself to be a perfect solution for the long-term monitoring of locomotor activity in different animal species [20]–[26]. In every application, the (terrestrial or aquatic) animal's dimensions and operative conditions determine the characteristics of the sensors, from the power of emission to the emission angle of the photobeam, and the viewing angle of the phototransistor.

The aim of the current work was to design a system able to monitor locomotor activity of a small marine nudibranch (*Melibe viridis*) and a freshwater cave decapod (*Typhlocaris salentina*). The small size of these animals (between 2 cm and 7 cm, with thin or transparent bodies) required a photobeam with a narrow angle of emission (maximum 10°) and a small diameter (3 mm). At the

same time, these animals need big aquaria (with 8 to 50 litres of capacity), the dimensions of which affect the IR LEDs with the characteristics aforementioned. IR LEDs do not work properly, or do not work at all, because of the attenuation effect of water on the photobeam.

We present our approach based on an infrared laser microbeam-emitter read by an NPN (Negative-Positive-Negative) phototransistor.

## 2. MATERIALS AND METHODS

### 2.1. General architecture of the system

Figure 1 and Figure 2 show the structure of the measurement bench specifically designed and realized for the experiment. In this version, the system is conceived for a laboratory use, where aquaria recreate the environmental conditions typically found in nature. When animals pass through the IR barrier blocking the light, this is transformed into an electric pulse that signals the movement. For these kinds of animals, considering their dimensions and behavior, and the dimensions of the aquaria, we realized two solutions. The first solution, a matrix of 4 x 3 IR barriers based on OPV300-OP598 (placed at the bottom, in the middle, and close to the surface of the aquarium) was used for *M. viridis*, a benthonic animal able to move along the smooth walls of the aquarium (Figure 1). The second solution, a single line of 3 IR barriers based on OPV332-OP598 (placed at the bottom of the aquarium), was realized for *T. salentina*, a benthonic animal that cannot move on the smooth walls of the aquarium (Figure 2). A smaller number would not allow us to gather enough data, while a higher number would not provide more information, needlessly complicating the circuit. A suitable electronic card then collects the pulses generated from the barriers. The signals undergo electrical conditioning to adapt them to the input dynamic range of the analogue-to-digital converter on the electronic boards.

### 2.2. Optoelectronic components

The discrete components selected to generate the IR barriers are the OPV300 [27], the OPV332 [28], and the OP598 [29], all manufactured by TT Electronics.

OPV300 is a high performance 850 nm infrared Vertical Cavity Surface-Emitting Laser (VCSEL). This product combines high-speed, high-output optical power and a concentric beam, making it an ideal transmitter for integration into all types of data communication equipment, as well as for reflective and transmissive switches. This device has been designed to be used for sensing applications, as well as air transmission of data, and the main characteristic is that the beam emission is perpendicular

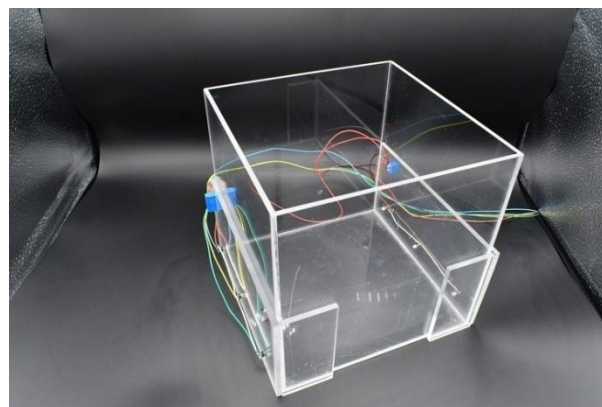


Figure 2. Electronic aquarium for *Typhlocaris salentina*.

from the top surface. This feature makes it particularly suitable for applications in which low current joined with high on-axis optical power must be ensured.

OPV332 is an infrared VCSEL, which, to obtain the same amount of output power, requires lower drive currents than LEDs, making it particularly suitable for low-power consumption applications such as battery-operated equipment. Nevertheless, for our application, the main characteristic is that the beam emission is perpendicular from the top surface. This is obtained by means of the dome lens packaging, which creates a narrow 4° beam angle from the device. Long distance applications benefit from this feature.

A cross-sectional view of the oxidized VCSEL is shown in Figure 3.

The VCSEL is driven by current: typically, the output is measured when the current exceeds a threshold, which is characteristic of each individual chip. The emitted angle is natively pretty narrow, but it can be even narrower with a dome lens (Figure 4).

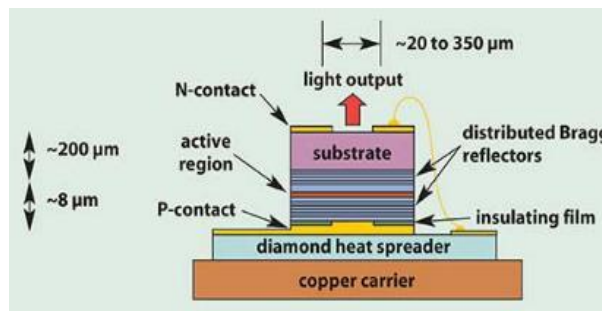


Figure 3. Cross-sectional view of the oxidized VCSEL.

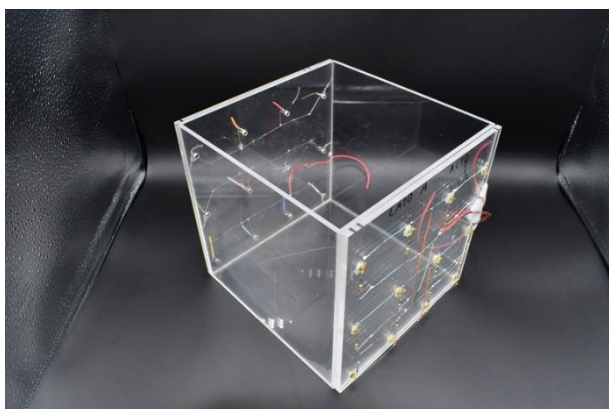


Figure 1. Electronic aquarium for *Melibe viridis*.

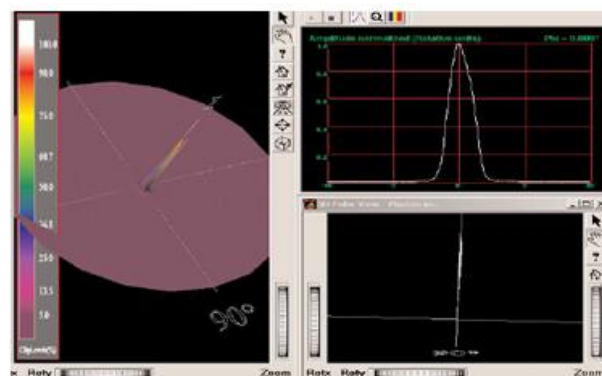


Figure 4. VCSEL – Dome Lens – Emission Diagram

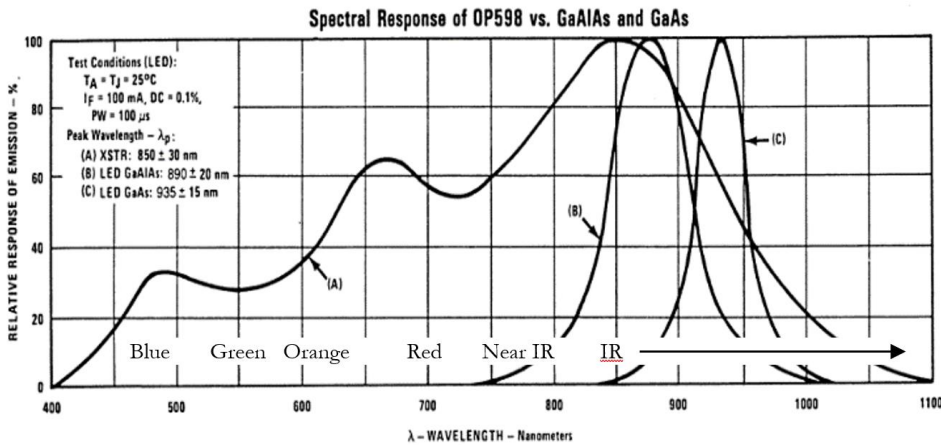


Figure 5. OP598 spectral relative response.

OP598 is an NPN phototransistor, in T1 package, specifically designed with a narrow receiving angle of 25°. The spectral relative response is shown in Figure 5.

The characteristics of OPV300/OPV332 and OP598 match the application requirements. In terms of being optical: the emitter and receiver both have narrow viewing and receiving angles, and narrow angles bring high accuracy levels; while the optical power of the VCSEL is what is necessary to avoid being absorbed by the water. The current consumption relative to the light output of the beam is very low.

### 2.3. Circuit

The output signal of each optoelectronic emitter-receiver couple is conditioned by an MC3303 operational amplifier [30], connected in a differential configuration. This configuration works as a current-voltage converter, allowing to convert the current of the photodiode stimulated by the absence of light into voltage. This is then amplified, making it suitable for the input dynamics of the successive digital stage. The signals coming from the IR couples are then sent to an OR gate (74LS21 [31]) used to sum all signals. The output of the OR gate is not directly connected to Raspberry-Pi GPIO (General Purpose Input Output) digital I/O pins. The signal coming from the OR is sent to an LM 555 [32] set in monostable mode. The latter provides an impulse of 15 ms limited to + 3.3 Vdc that is compatible with GPIO input dynamics. Figure 6 shows a schematic view of the signal conditioning circuit reduced to only two IR sensors.

Temporal resolution is a trade-off between the need to continuously monitor the movements and the real animal motion; experimentally estimated for these kinds of animals to be equal to 15 ms and + 3.3 Vdc, so that compatibility with the GPIO input dynamics is ensured.

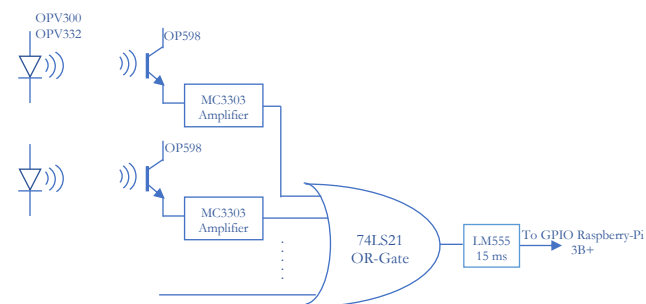


Figure 6. Schematic of the signal conditioning stage.

A Raspberry-Pi [33] model 3B+ is placed at the end of the measurement chain. It has a 64-bit quad-core processor running at 1.4 GHz, and it represents a perfect compromise between technical needs, costs, and ease of use.

Technically, its hardware features make this device suitable for all those measurements in which the variability of the parameter under investigation is low-frequency. However, the functional feature that makes it a winner is the large availability of open libraries and the possibility of programming it in a high-level programming language such as Python. This prerogative,

from a technical point of view, is certainly an advantage, but the most important thing is the reconfigurability of the system with relative ease, even for non-experts in hardware and software. Hardware features include a dual-band 2.4 GHz and 5 GHz wireless LAN, Bluetooth 4.2/BLE, Gigabit Ethernet over USB 2.0, and a PoE capability via a separate PoE HAT. The dual-band wireless LAN comes with modular compliance certification. The mechanical footprint Raspberry Pi 3 Model B+ is like that of previous models such as Raspberry Pi 2 Model B and Raspberry Pi 3 Model B.

### 2.4. Software

The system presented here is conceived for both field and laboratory applications. The computing capacity of Raspberry is suitable to manage data acquisition and data analysis, however, considering the particular laboratory application, we preferred to separate both stages, with the data analysis being successively performed on a personal computer. All the data analysis routines are already set to provide the locomotor activity of the animals in the computer.

The acquisition software executes iterative indented time-based multi-level cycles, the structure of which is shown in the flow chart in Figure 7. In the nucleus of the program, a cycle of 50 ms is set to read the pin connected to the conditioning stage. Only a high level on the pin will indicate that the animal passed through the IR barriers. If the pin is high, an internal software counter is increased. Every minute the data counter is saved in a text file. This period is called the sampling frequency, and it is usually set to 1 minute, in order to have a high data resolution. This high resolution is not needed to study circadian rhythms, but it is very useful for the ultradian rhythms in the range of

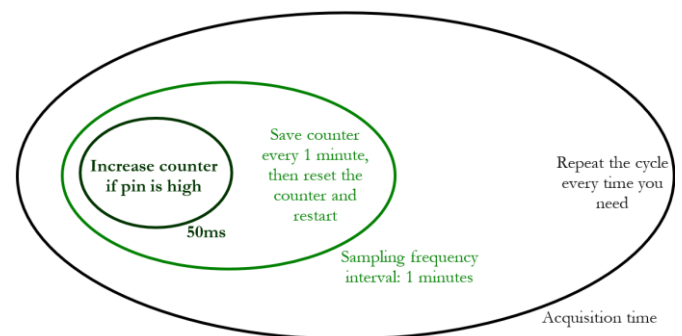


Figure 7. Flow chart of the acquisition software.

minutes or hours. Acquisition time is the length of time (minutes, hours, or days) over which we want to repeat the sampling cycle. In order to study the circadian rhythm, we typically consider 8–10 days. Both the sampling frequency and the acquisition time could theoretically and technically be modified as desired, but this choice depends on the granularity of the successive data analysis, which, in order to be consistent, needs to respect the chronobiological constraints [34].

### 2.5. Experimental phase

A preliminary experiment was conducted in order to test the device and software. This experiment merely aimed to determine if the system detects animals' movement and the chronobiological profile of their behaviour.

Marine and freshwater invertebrates chosen for this research will be the object of future studies.

We analysed the activity of *Melibe viridis*, in Figure 8, a non-indigenous nudibranch, collected in October 2024 in Mar Piccolo Taranto (Taranto, Italy), using a hand-net during scuba dive, and stored in a 10-litre plastic tank. The second species is a cave-dwelling shrimp, *Typhlocaris salentina* (Caroli, 1923), in Figure 9, an endemic species of Salento, collected in the "Cunicolo del Diavolo" (LE, Pu/101 - Otranto, Italy), using a hand-net, and stored in a 10-litre plastic tank.



Figure 8. *Melibe viridis*.



Figure 9. *Typhlocaris salentina*.

### 2.6. Experimental procedure

After capture, the animals were carried to the laboratory, where they were immediately and individually transferred into an 8-litre plastic tank ( $20 \times 20 \times 20 \text{ cm}^3$ ) at the temperature of  $(18 \pm 1) \text{ }^\circ\text{C}$ . *Melibe viridis* was then exposed to a light-dark cycle (LD12:12) and *T. salentina* to continuous darkness (DD). The aquaria lacked pumps for the circulation and filtration of water, to avoid interference with the electronic monitoring system. Animals were kept using the water collected during the sampling.

No food was provided during the tests to prevent the synchronization of activity rhythms upon feeding timing. Animals were monitored continuously for two days with a record every 1 minute.

The device counted the number of photobeam interruptions every minute, storing this information and a timestamp in a file.

### 2.7. Data analysis

Although for this test we only recorded for two days, which is not sufficient for a complete chronobiological profile of the animals, we proceeded with the analysis.

Qualitative analysis included a daily and hourly representations of the activity, using a double-plot actogram, while quantitative analysis comprised the total amount of locomotor activity, mean hourly locomotor activity, and Lomb–Scargle periodogram in the range of 13–30 hours.

In order to analyse the data, we used Calc, an Open Office spreadsheet for computation, and RhythmicAlly, an open-source program using R and Shiny. Statistical significance was set to  $p = 0.05$ .

## 3. RESULTS AND DISCUSSION

A simple visual check of the files showed the detection of the locomotor activity in both animals.

A qualitative analysis by a double plot actogram showed a daily concentration of the activity for *M. viridis*, while it did not show any in *T. salentina* (Figure 10, left side).

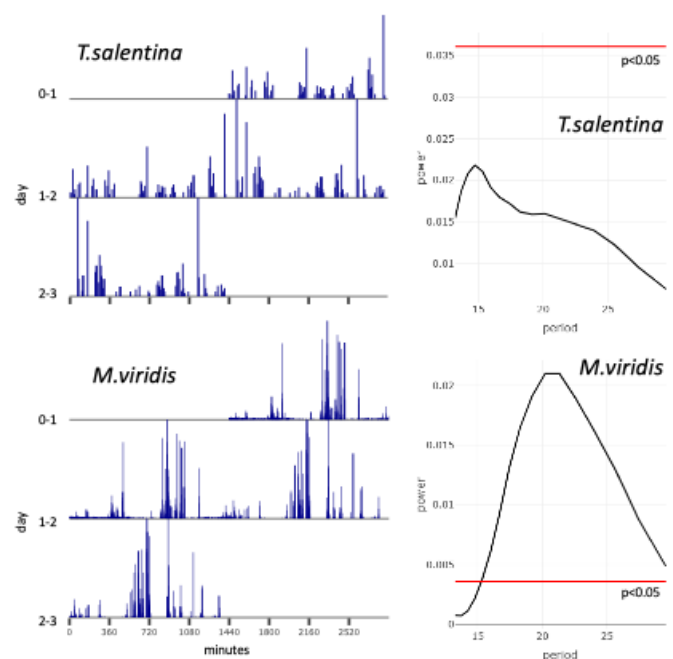


Figure 10. On the left side the double-plot actograms (two days per line). On the right side the periodograms, the red lines show the significant level for  $p < 0.05$ .

In order to quantify the locomotor activity, we calculated the amount of activity during the 48 hours of monitoring. In total, we recorded 6,951 photobeam interruptions for *M. viridis* ( $48.1 \pm 56.5$ , mean  $\pm$  SD), with an average of 2.41 per minute, and a total of 1,171 photobeam interruption for *T. salentina* ( $7.5 \pm 8.1$ , mean  $\pm$  SD), with an average of 0.41 per minute.

As the last analysis, we verified the presence of circadian rhythmicity by Lomb–Scargle periodogram in the range of 13–30 hours. As showed by the actogram, a circadian rhythm was present in *M. viridis*, while *T. salentina* did not show circadian rhythms (Figure 10, right side).

The system presented and tested here is based on the changes made on the system previously developed for *Lepidurus arcticus* [35] and *Gammarus setosus* [36]. We maintained the same electronic circuit, but changed the optical sensors based on an infrared VCSEL laser barrier.

Our results showed that the optical system and the electronic coupling with the old circuit are able to detect the movement in small aquatic animals inside medium and big aquaria.

From an ethological point of view, these results show that the device can be useful to monitor the locomotor activity, including long-term monitoring needed to characterize the chronobiological parameters of these animals.

We constructed an affordable system, which monitors the locomotor activity of aquatic animals without interfering with the animals' behavior. The developed system has a logical and electronic simplicity that offers great flexibility, and it is easily expandable. It is important to notice that the system is not limited, and it can be used in other biological applications on behavioral and physiological monitoring, solving and offering a technology non-existent in the market. Our work here makes high-throughput animal behavior monitoring accessible to a broad range of scientists.

The entire system is constructed with commercially available and affordable components. Our approach is based on open-source hardware and software that can be shared among the scientific community for user-defined application and further development. The use and development of open-source software are encouraged by the European Commission to foster innovation by sharing knowledge and expertise, and it is a solution to a democratic access to science [37].

#### 4. CONCLUSIONS

In conclusion, we found the IR-actuated movement detector to be a highly sensitive and reliable device, in spite of its relatively modest cost. It is appropriate to a wide range of experimental protocols and data-recording systems. However, given the ease with which simple infrared sensors can be implemented, investigators would be wise to consider making their own, rather than purchasing functionally equivalent and much more expensive commercial sensors.

#### AUTHORS' CONTRIBUTION

Conceptualization by VP and FL. Investigation by VP. Methodology by VP and FL. Software by FL. Electronic resources by NC. Formal analysis by VP. Visualization by VP, NC and FL. Writing original draft and editing by VP, NC, and FL.

#### ACKNOWLEDGEMENTS

Pietro Fermani and Pietro Creti for the electronic circuit. Giulia Furfaro and Michele Solca for collecting and maintaining nudibranch *Melibe viridis*. Salvatore Inguscio and Francesco Cozzoli for collecting and maintaining *Typhlocaris salentina*. Alberto Basset and Fabio Vignes for laboratory facilities. MD SRL and RS Components for the support.

#### REFERENCES

- [1] A. Rogalski, History of infrared detectors, *Opto-Electron Rev.*, vol. 20, 2012, pp. 279–308.
- [2] A. I. Dell, J. A. Bender, K. Branson, I. D. Couzin, G. G. de Polavieja, L. P. J. J. Noldus, A. Pérez-Escudero, P. Perona, A. D. Straw, M. W. Wikelski, U. Brose, Automated image-based tracking and its application in ecology, *Trends in Ecology & Evolution*, vol. 29, 2014, pp. 417–428. DOI: [10.1016/j.tree.2014.05.004](https://doi.org/10.1016/j.tree.2014.05.004)
- [3] H. C. Fibiger, G. S. Lynch, H. P. Cooper, A biphasic action of central cholinergic stimulation non behavioral arousal in the rat, *Psychopharmacologia*, vol. 20, 1971, pp. 366–382.
- [4] E. Zakharova, G. Leoni, I. Kichko, S. Izenwasser, Differential effects of methamphetamine and cocaine on conditioned place preference and locomotor activity in adult and adolescent male rats, *Behavioural Brain Research*, vol. 198, 2009, pp. 45–50. DOI: [10.1016/j.bbr.2008.10.019](https://doi.org/10.1016/j.bbr.2008.10.019)
- [5] M. A. Geyer, P. V. Russo, D. S. Segal, R. Kuczenski, Effects of apomorphine and amphetamine on patterns of locomotor and investigatory behavior in rats, *Pharmacology, Biochemistry and Behaviour*, vol. 28, 1987, pp. 393–399. DOI: [10.1016/0091-3057\(87\)90460-6](https://doi.org/10.1016/0091-3057(87)90460-6)
- [6] J. E. Gresack, V. B. Risbrough, C. N. Scott, S. Coste, M. Stenzel-Poore, M. A. Geyer, S. B. Powell, Isolation rearing-induced deficits in contextual fear learning do not require CRF(2) receptors, *Behavioural Brain Research*, vol. 209, 2010, pp. 80–84. DOI: [10.1016/j.bbr.2010.01.018](https://doi.org/10.1016/j.bbr.2010.01.018)
- [7] E. P. Riley, N. R. Shapiro, E. A. Lochry, Nose-poking and head-dipping behaviors in rats prenatally exposed to alcohol, *Pharmacology, Biochemistry and Behaviour*, vol. 11, 1979, pp. 513–519. DOI: [10.1016/0091-3057\(79\)90034-0](https://doi.org/10.1016/0091-3057(79)90034-0)
- [8] D. Dietz, H. Wang, M. Kabbaj, Corticosterone fails to produce conditioned place preference or conditioned place aversion in rats, *Behavioural Brain Research*, vol. 181, 2007, pp. 287–291. DOI: [10.1016/j.bbr.2007.04.005](https://doi.org/10.1016/j.bbr.2007.04.005)
- [9] J. W. Jahng, T. A. Houpt, MK801 increases feeding and decreases drinking in non deprived, freely feeding rats, *Pharmacology, Biochemistry and Behaviour*, vol. 68, 2001, pp. 181–186. DOI: [10.1016/S0091-3057\(00\)00434-2](https://doi.org/10.1016/S0091-3057(00)00434-2)
- [10] Y. Kurylyak, K. Barbè, (+ 4 more authors), Photoplethysmogram-based Blood pressure evaluation using Kalman filtering and Neural Networks, *proc. of MeMeA 2013 - IEEE International Symposium on Medical Measurements and Applications*, 2013, pp. 170–174. DOI: [10.1109/MeMeA.2013.6549729](https://doi.org/10.1109/MeMeA.2013.6549729)
- [11] F. Lamonaca, D. L. Carnì, (+ 4 more authors), Blood oxygen saturation measurement by smartphone camera, *proc. of IEEE International Symposium on Medical Measurements and Applications*, MeMeA, 2015, pp. 359–364. DOI: [10.1109/MeMeA.2015.7145228](https://doi.org/10.1109/MeMeA.2015.7145228)
- [12] M. Ceccarelli, A. Speranza, D. Grimaldi, F. Lamonaca, Automatic detection and surface measurements of micronucleus by a computer vision approach, *IEEE Transactions on Instrumentation and Measurement*, vol. 59, No. 9, 2010, pp. 2383–2390. DOI: [10.1109/TIM.2010.2049184](https://doi.org/10.1109/TIM.2010.2049184)
- [13] P. Daponte, P. Picariello, (+ 4 more authors), A Survey of Measurement Applications Based on IoT, *proc. of Workshop on Metrology for Industry 4.0 and IoT, MetroInd 4.0 and IoT*, 2018,

- pp. 157–162.  
DOI: [10.1109/METRO14.2018.8428335](https://doi.org/10.1109/METRO14.2018.8428335)
- [14] E. Balestrieri, L. De Vito, (+ 4 more authors), Research challenges in Measurements for Internet of Things systems, *Acta IMEKO*, vol. 7, No. 4, 2018, pp. 82–94.  
DOI: [10.21014/acta\\_imeko.v7i4.675](https://doi.org/10.21014/acta_imeko.v7i4.675)
- [15] S. A. Pullano, A. S. Fiorillo, (+ 3 more authors), Comprehensive system for the evaluation of the attention level of a driver, 2016 IEEE Int. Symp. on Medical Measurements and Applications, MeMeA, 2016, pp. 1–5.  
DOI: [10.1109/MeMeA.2016.7533710](https://doi.org/10.1109/MeMeA.2016.7533710)
- [16] M. T. Verde, P. Guerriero, (+ 6 more authors), A measurement system for enteric CH<sub>4</sub> emissions monitoring from ruminants in livestock farming, *Acta IMEKO*, vol. 12, No. 4, 2023, pp. 1–6.  
DOI: [10.21014/actaimeko.v12i4.1618](https://doi.org/10.21014/actaimeko.v12i4.1618)
- [17] R. A. Guerròn, F. D'Amore, (+ 5 more authors), IoT sensor nodes for air pollution monitoring: A review, *Acta IMEKO*, vol. 12, No. 4, 2023, pp. 1–10.  
DOI: [10.21014/actaimeko.v12i4.1676](https://doi.org/10.21014/actaimeko.v12i4.1676)
- [18] I. Ahmed, E. Balestrieri, (+ 5 more authors), Morphometric Measurement of Fish Blood Cell: An Image Processing and Ellipse Fitting Technique, *IEEE Transactions on Instrumentation and Measurement*, vol. 73, 2024, pp. 1–12.  
DOI: [10.1109/TIM.2024.3353280](https://doi.org/10.1109/TIM.2024.3353280)
- [19] S. Siciliano, C. G. Lopresto, F. Lamonaca, From traditional packaging to smart bio-packaging for food safety: a review, *Euro-Mediterranean Journal for Environmental Integration*, vol. 9, No. 4, 2024, pp. 1971–1986.  
DOI: [10.1007/s41207-024-00627-8](https://doi.org/10.1007/s41207-024-00627-8)
- [20] D. Sarriá, J. D. Río, (+ 4 more authors), Actographic detection system based on infrared and computer vision technologies to measure the behaviour of species, *Proc. of the 16th IMEKO TC4 Int. Symp.*, Florence, Italy, 22-24 September 2008. Online [Accessed 19 October 2025]  
<https://www.imeko.org/publications/tc4-2008/IMEKO-TC4-2008-004.pdf>
- [21] S. H. Simonetta, D. A. Golombek, An automated tracking system for *Caenorhabditis elegans* locomotor behavior and circadian studies application, *Journal Neuroscience Methods*, vol. 161(2), 2007, pp. 273–280.  
DOI: [10.1016/j.jneumeth.2006.11.015](https://doi.org/10.1016/j.jneumeth.2006.11.015)
- [22] V. Pasquali, P. Renzi, G. Belmonte, G. L. Pesce, An infra-red beam device for the study of the motor activity rhythms in groundwater mysidacea, *Thalassia Salentina*, vol. 30, 2007, pp. 93–106. Online [Accessed 15 May 2025]  
<http://siba-ese.unisalento.it/index.php/thalassiasal/article/view/2296>
- [23] V. Pasquali, Locomotor activity rhythms in high arctic freshwater crustacean: *Lepidurus arcticus* (Branchiopoda; Notostraca), *Biological Rhythm Research*, vol. 46(3), 2015, pp. 453–458.  
DOI: [10.1080/09291016.2015.1004842](https://doi.org/10.1080/09291016.2015.1004842)
- [24] A. E. McLelland, C. E. Winkler, M. T. Martin-Iverson, A simple and effective method for building inexpensive infrared equipment used to monitor animal locomotion, *Journal of Neuroscience Methods*, vol. 243, 2015, pp. 1–7.  
DOI: [10.1016/j.jneumeth.2015.01.006](https://doi.org/10.1016/j.jneumeth.2015.01.006)
- [25] V. Pasquali, G. D'Alessandro, R. Gualtieri, F. Leccese, A new data logger based on Raspberry-Pi for Arctic *Notostraca* locomotion investigation, *Measurement*, vol. 110, 2017, pp. 249–256.  
DOI: [10.1016/j.measurement.2017.07.004](https://doi.org/10.1016/j.measurement.2017.07.004)
- [26] Q. Tang, S. P. Williams, A. D. Güler, A building block-based beam-break (B5) locomotor activity monitoring system and its use in circadian biology research, *BioTechniques*, vol. 73, 2022, pp. 104–109.  
DOI: [10.2144/btn-2022-0036](https://doi.org/10.2144/btn-2022-0036)
- [27] OPTEK, OPV300 Datasheet. Online [Accessed 15 May 2025]  
<https://www.ttelectronics.com/TTElectronics/media/ProductFiles/Datasheet/OPV300-310Y-314Y.pdf>
- [28] OPTEK, OPV332 Datasheet. Online [Accessed 15 May 2025]  
<https://www.mouser.it/datasheet/2/414/OPV332-3241440.pdf>
- [29] OPTEK, OP598B Datasheet. Online [Accessed 15 May 2025]  
[http://pdf.datasheetcatalog.com/datasheet\\_pdf/optek-technology/OP593A\\_to\\_OP598C.pdf](http://pdf.datasheetcatalog.com/datasheet_pdf/optek-technology/OP593A_to_OP598C.pdf)
- [30] Texas Instruments, MC3303 Datasheet. Online [Accessed 15 May 2025]  
<http://www.ti.com/product/mc3303>
- [31] Texas Instruments, 74LS21 Datasheet. Online [Accessed 15 May 2025]  
<http://www.futurlec.com/74LS/74LS21.shtml>
- [32] Texas Instruments, MC3303 Datasheet. Online [Accessed 15 May 2025]  
<http://www.ti.com/product/LM555>
- [33] J. Jolles, Broad-scale applications of the Raspberry Pi: A review and guide for biologists, *Methods in Ecology and Evolution*, vol. 12(9), 2021, pp. 1562–1579.  
DOI: [10.1111/2041-210X.13652](https://doi.org/10.1111/2041-210X.13652)
- [34] R. Refinetti, Laboratory instrumentation and computing: comparison of six methods for the determination of the period of circadian rhythms, *Physiology & Behaviour*, vol. 54, 1993, pp. 869–875.  
DOI: [10.1016/0031-9384\(93\)90294-P](https://doi.org/10.1016/0031-9384(93)90294-P)
- [35] V. Pasquali, R. Gualtieri, G. D'Alessandro, F. Leccese, M. Cagnetti, Experimental in field reliability test for data logger based on Raspberry-Pi for extreme scenarios: A first step versus aerospace applications, *IEEE Metrology for Aerospace*, pp. 365–370.  
DOI: [10.1109/MetroAeroSpace.2016.7573242](https://doi.org/10.1109/MetroAeroSpace.2016.7573242)
- [36] V. Pasquali, R. Gualtieri, G. D'Alessandro, M. Granberg, D. Hazlerigg, M. Cagnetti, F. Leccese, Monitoring and analyzing of circadian and ultradian locomotor activity based on Raspberry-Pi, *Electronics* vol. 5, 2016, p. 58.  
DOI: [10.3390/electronics5030058](https://doi.org/10.3390/electronics5030058)
- [37] M. Oellermann, J. W. Jolles, D. Ortiz, R. Seabra, T. Wenzel, H. Wilson, R. L. Tanner, *Open Hardware in Science: The Benefits of Open Electronics*, *Integrative & Comparative Biology*, vol. 62(4), 2022, pp. 1061–1075.  
DOI: [10.1093/icb/icac043](https://doi.org/10.1093/icb/icac043)